

Interfacial Electrostatic Interaction Overcomes Backward Electron Transfer without CrO_x-Based Core–Shell Cocatalyst for Efficient Z-Scheme Water Splitting

Ren Itagaki, Akinobu Nakada,* Hajime Suzuki, Osamu Tomita, and Ryu Abe*



Cite This: <https://doi.org/10.1021/jacs.5c23111>



Read Online

ACCESS |



Metrics & More



Article Recommendations



Supporting Information

ABSTRACT: Z-scheme water splitting with a redox mediator, which transports electrons from an H₂- to an O₂-evolving photocatalyst, has been widely studied to achieve efficient overall water splitting. However, backward electron transfer with the redox mediator is an intrinsic drawback of Z-scheme water splitting, because it interrupts the desired H₂ and O₂ evolution. Although a CrO_x shell coating on metal cocatalysts on an H₂-evolving photocatalyst is widely used to block backward electron transfer, this strategy relies on potentially toxic chromium species of which elution is possible under the photocatalytic operation. Herein, we demonstrate a chromium-free approach that suppresses backward electron transfer by manipulating electrostatic interactions at the photocatalyst–mediator interface. The designed charge-switchable cobalt complex serves as a superior mediator that selectively suppresses backward electron transfer from a positively charged H₂-evolving photocatalyst without using a CrO_x shell, leading to efficient Z-scheme water splitting with an apparent quantum yield of 7.2%.

Z-scheme water splitting using semiconductor photocatalysts has been extensively studied to produce H₂ as energy and chemical resources.^{1–4} In a typical Z-scheme configuration, two distinct semiconductor photocatalysts for H₂ or O₂ evolution are interconnected via a reversible electron mediator (redox couple) in solution (Figure 1a).^{4–6} Although this architecture allows the use of various kinds of visible-light-responsive photocatalysts, an inherent drawback of the Z-scheme system is its competitive backward electron transfer reactions.⁴ Because the redox potential of the mediator must lie between the conduction band minimum of the O₂-evolving photocatalyst and the valence band maximum of the H₂-evolving photocatalyst, backward electron transfer from the HEP to the OEP via the mediator is thermodynamically unavoidable (Figure 1a), decreasing the overall photocatalytic efficiency.

To suppress the backward reactions, cocatalyst engineering has been demonstrated as the main strategy.^{7–10} Specifically, for the H₂-evolving catalyst center, CrO_x shell coating on metal cocatalysts is the most widely applied approach to selectively suppress the undesirable reduction of redox species and H₂ combustion with O₂ to enable selective proton reduction.^{7,11–15} The role of the CrO_x shell has been reported as a blocker for molecular redox mediators (e.g., IO₃[−], [Co(bpy)₃]³⁺, Fe³⁺, [Fe(CN)₆]^{3−}, [SiVW₁₁O₄₀]^{5−}) and O₂, while it accepts the penetration of the proton to the metal catalyst centers (Figure 1b).^{7,11,16} Therefore, the CrO_x shell has been employed in efficient photocatalytic water splitting systems so far.^{7,11,12,17–19}

However, the CrO_x shell approach has several drawbacks (Figure 1b). The first concern is the dissolution of chromium species to the environment,^{11,20–22} including toxic hexavalent Cr generated via photooxidation of CrO_x.^{21,22} Some reports

have shown that the CrO_x shell decreases the rate of proton reduction catalysis, which is a trade-off for resistance to backward reactions.^{12,19} Furthermore, the CrO_x shell is typically coated on metal cocatalyst nanoparticles selectively via photodeposition techniques.¹⁷ Therefore, it is essentially difficult to shut out the backward transfer of photoexcited electrons on the bare photocatalyst surface before reaching the cocatalyst (Figure 1b). These facts motivated us to develop an alternative strategy to suppress backward electron transfer without the aid of CrO_x shells to boost overall Z-scheme water splitting.

Herein, we demonstrate a strategy to suppress backward electron transfer by manipulating the electrostatic interaction between the photocatalyst surface and a redox mediator. The strong effects of introducing a neutral/cationic charge-switchable cobalt complex [Co(bpc)₂]⁺⁰ (bpc = 2,2'-bipyridine-6-carboxylate) as the electron mediator and appropriate surface charges to enable efficient Z-scheme photocatalytic water splitting even without CrO_x shells are discussed (Figure 1c).

The charge-switchable cobalt complex [Co(bpc)₂]⁺⁰ (¹H NMR: Figure S1) exhibited reversible redox behavior at +0.25 V vs Ag/AgCl and was independent over a range of pH 2.0–9.5 (Figure S2). As a benchmark, this study employed rhodium-doped SrTiO₃ (denoted as SrTiO₃:Rh) and cesium-

Received: December 24, 2025

Revised: February 10, 2026

Accepted: February 12, 2026

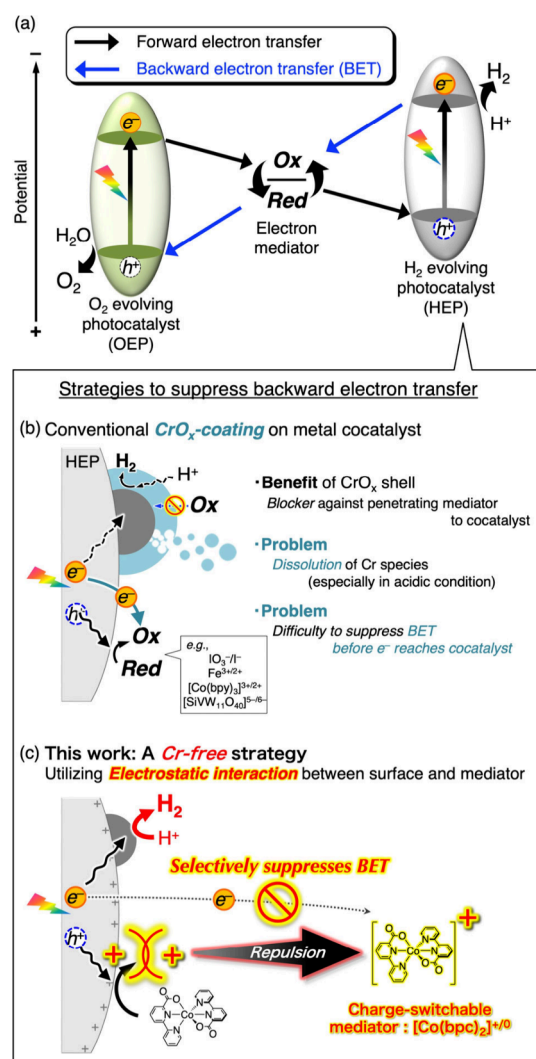


Figure 1. (a) Schematic illustration of the Z-scheme water splitting system using a redox mediator. Approaches for overcoming backward electron transfer by the (b) conventional CrO_x shell strategy and (c) strategy of this work.

modified WO_3 (denoted as WO_3) as H_2 - and O_2 -evolving photocatalysts,^{23,24} respectively (Figure S3).

Figure 2 shows the time courses of H_2 evolution over CrO_x /Ru/SrTiO₃:Rh and Ru/SrTiO₃:Rh using the redox-reversible $[Co^{II}(bpc)_2]^0$ as an electron donor. At pH 6.0, the CrO_x shell

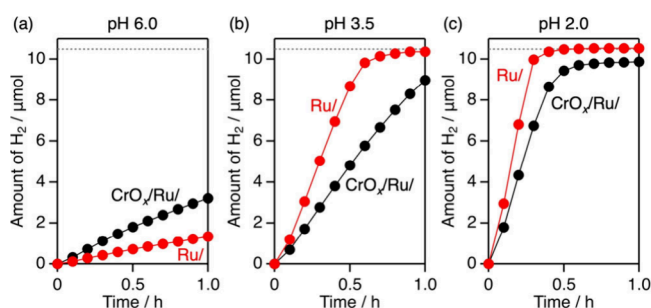


Figure 2. Time courses of H_2 evolution using CrO_x /Ru or Ru-loaded SrTiO₃:Rh in an aqueous solution (10 mg in 70 mL) containing 0.3 mM $[Co^{II}(bpc)_2]^0$ at different solution pH under visible-light irradiation ($\lambda = 430$ nm).

coating provided higher H_2 evolution rates than the uncoated Ru cocatalyst. The CrO_x shell coating rarely affected the H_2 evolution activity when MeOH was used as an irreversible electron donor instead of $[Co^{II}(bpc)_2]^0$ (Figure S4). Hence, the promotional effect of the CrO_x shell observed at pH 6.0 can be concluded as a blocker toward backward electron transfer to its oxidized counterpart $[Co^{III}(bpc)_2]^+$, similar to previous reports for conventional redox mediators.^{7,11,16} In contrast, the uncoated Ru cocatalyst induced higher H_2 evolution rates under acidic conditions than those on CrO_x -coated ones. This finding strongly suggests the presence of another mechanism for suppressing backward electron transfer to the oxidized $[Co^{III}(bpc)_2]^+$ species. The best H_2 evolution activity was recorded as 7.1% of the apparent quantum yield (AQY) at 430 nm by using Ru/SrTiO₃:Rh in the presence of a $[Co^{II}(bpc)_2]^0$ electron donor at pH 2.0.

To evaluate the resistance to backward electron transfer, the effects of adding the oxidized form $[Co^{III}(bpc)_2]^+$ on photocatalytic H_2 evolution were investigated (Table 1). At pH 6.0, the CrO_x coating on Ru/SrTiO₃:Rh exhibited superior resistance to decreasing the H_2 evolution rate upon the addition of $[Co^{III}(bpc)_2]^+$, leading to higher photocatalytic activity than the uncoated Ru/SrTiO₃:Rh photocatalyst (Entries 1 and 4). This suggests that the CrO_x coating served as a blocker for backward electron transfer on Ru cocatalyst at pH 6.0. When pH decreased to 3.5 and 2.0, the resistance to backward electron transfer improved overall, of which exposed Ru/SrTiO₃:Rh was comparable to or even better than CrO_x /Ru/SrTiO₃:Rh (Table 1). Importantly, zeta potentials of the SrTiO₃:Rh samples were negative at pH 6.0 but increased and flipped to positive in the acidic solution (Table 1). This relationship implies that the electrostatic interaction between the photocatalyst surface and the redox mediator plays a key role in suppressing backward electron transfer.

$[Co^{II}(bpc)_2]^0$ ($E_{1/2} = 0.25$ V vs Ag/AgCl; Figure S2) can thermodynamically supply electrons to photoexcited SrTiO₃:Rh photocatalyst (potential of $Rh^{4+/3+}$ state is 1.90 V vs Ag/AgCl^{25,26} at pH 2.0), resulting in the transformation to cationic $[Co^{III}(bpc)_2]^+$ as the oxidized form during photocatalytic H_2 evolution. If the zeta potential of the SrTiO₃:Rh photocatalyst is negative (at pH 6.0), then the generated $[Co^{III}(bpc)_2]^+$ would be electrostatically attracted, likely accelerating backward electron transfer (Figure 3a). Therefore, the H_2 evolution rate was highly sensitive to the coexistence of $[Co^{III}(bpc)_2]^+$ at pH 6.0. Notably, although the CrO_x shell played a role in resisting backward electron transfer, the H_2 evolution rates decreased by 45% at pH 6.0 (Entry 1 in Table 1). This may be attributed to the occurrence of backward electron transfer on the SrTiO₃:Rh surface before the photoexcited electrons reached the cocatalyst even in the presence of CrO_x coating on the Ru cocatalyst.

Compared with the results at pH 6.0, the deactivation of H_2 evolution by the addition of $[Co^{III}(bpc)_2]^+$ was significantly suppressed, regardless of the presence or absence of the CrO_x shell under acidic conditions, where the zeta potential of SrTiO₃:Rh was positive (Table 1). Positive zeta potentials would induce electrostatic repulsion with $[Co^{III}(bpc)_2]^+$, which likely decreased the opportunity for backward electron transfer (Figure 3b). H_2 evolution rates were further improved by decreasing the pH from 3.5 to 2.0, where the proton concentration, zeta potential, and driving force of forward electron transfer from $[Co^{II}(bpc)_2]^0$ were increased. Remarkably, Ru/SrTiO₃:Rh exhibited highly efficient H_2 evolution,

Table 1. Summary of Surface Property and H₂ Evolution Activity of SrTiO₃:Rh Photocatalysts

Entry	Cocatalyst	pH	Zeta potential (mV)	H ₂ evolution rate (r_{H_2}) ^a ($\mu\text{mol h}^{-1}$)		Activity retention ratio ^d (%)	CrO _x dissolution ^e (%)
				$r_{\text{H}_2}(\text{Co}^{\text{II}})$ ^b	$r_{\text{H}_2}(\text{Co}^{\text{II}} + \text{Co}^{\text{III}})$ ^c		
1	CrO _x /Ru	6.0	-17.7	4.0	2.2	55	0
2		3.5	+40.4	10.6	8.8	83	0.4
3		2.0	+44.2	25.2	18.3	73	20
4	Ru	6.0	-25.2	1.4	0.7	50	—
5		3.5	+39.9	19.8	12.7	64	—
6		2.0	+55.6	38.6	33.7	87	—

^aInitial rate recorded by irradiation of 430 nm light to an aqueous dispersion (70 mL) containing a SrTiO₃:Rh photocatalyst (10 mg) and Co complexes (0.3 mM each). ^bRate in the presence of [Co^{II}(bpc)₂]⁰. ^cRate in the presence of [Co^{II}(bpc)₂]⁰ and [Co^{III}(bpc)₂]⁺. ^dEstimated by $r_{\text{H}_2}(\text{Co}^{\text{II}} + \text{Co}^{\text{III}})/r_{\text{H}_2}(\text{Co}^{\text{II}})$. ^eDetermined by ICP-OES (see Table S1).

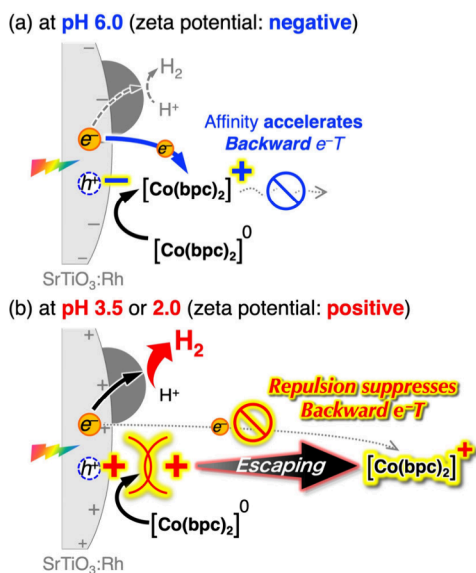


Figure 3. Plausible schematic illustration of photoinduced electron transfer and backward electron transfer processes with (a) a negatively- or (b) a positively-charged surface.

even better than CrO_x/Ru/SrTiO₃:Rh (Entries 2, 3, 5, and 6). One possible reason is that the CrO_x shell also blocks the proton reduction, as previously reported.^{12,19} The partial dissolution of chromium species was observed at pH 2.0 (Entry 3 in Table 1, Table S1). One can notice that H₂ evolution at pH 2.0 using CrO_x/Ru/SrTiO₃:Rh stopped at 9.0 μmol , which is below the stoichiometric limit (10.5 μmol), assuming the consumption of the [Co^{II}(bpc)₂]⁰ electron donor (Figure 2c). These results suggest that CrO_x shells are chemically unstable at low pH,¹¹ which is one of the most serious concerns when using CrO_x shells.

The superior H₂ evolution activity of Ru/SrTiO₃:Rh against CrO_x/Ru/SrTiO₃:Rh was not observed when a conventional polyoxometalate ([SiV^{IV}W₁₁O₄₀]^{5-/6-}) mediator was applied (Figure 4a-c), similar to previous reports on CrO_x shell for conventional mediators.^{7,11} In the case of anionic mediators, the anionic oxidized form (i.e., [SiV^VW₁₁O₄₀]⁵⁻) generated by the photoinduced electron transfer to SrTiO₃:Rh should feel an electrostatic affinity for the positively charged SrTiO₃:Rh surface. Hence, the CrO_x shell was essential to showing superior photocatalytic activity in the case of anionic mediators. We can conclude that the appropriate manipulation of the interfacial electrostatic interaction with the designed neutral/cation-switchable [Co(bpc)₂]⁺⁰ is effective in suppressing backward electron transfer without decelerating

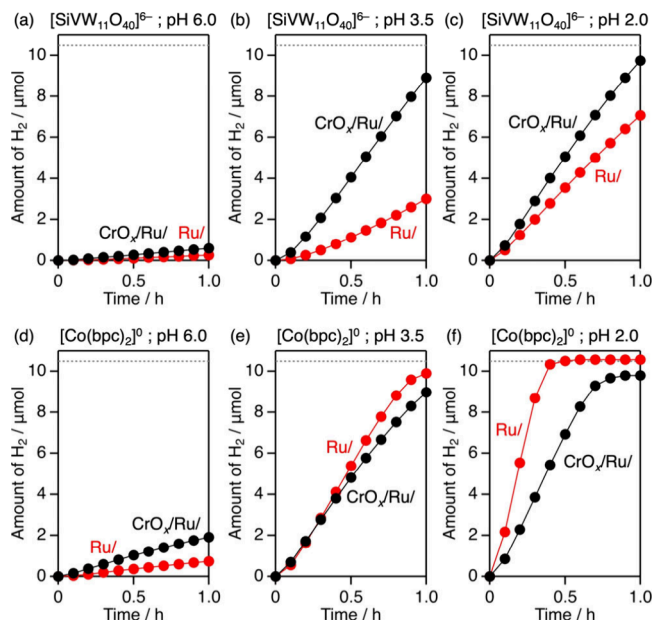


Figure 4. Time courses of H₂ evolution using Ru/SrTiO₃:Rh or CrO_x/Ru/SrTiO₃:Rh (10 mg) in an aqueous solution (70 mL) containing (a,b,c) [SiV^{IV}W₁₁O₄₀]⁶⁻ and [SiV^VW₁₁O₄₀]⁵⁻ and (d,e,f) [Co^{II}(bpc)₂]⁰ and [Co^{III}(bpc)₂]⁺ (0.3 mM each) at various pH under visible-light irradiation ($\lambda = 430$ nm).

forward reactions, leading to highly efficient H₂ evolution without the aid of the CrO_x shell.

Figures 5 and S5 show the time courses of Z-scheme water splitting using Ru-loaded SrTiO₃:Rh with PtO_x/WO₃ and various redox mediators at pH 2.0. Compared with benchmark redox mediators,²⁷⁻³⁰ the [Co^{III}(bpc)₂]⁺/[Co^{II}(bpc)₂]⁰ system induced the highest rate of water splitting (Figure 5a). The rate of water splitting was even higher than that using the CrO_x shell (Figure 5b). Note that obvious reverse water formation from H₂ and O₂ was not observed even without a CrO_x shell (Figure S6). The AQY of 7.2% was recorded at 405 nm for the overall water splitting with the Ru/SrTiO₃:Rh-[Co^{III}(bpc)₂]⁺/[Co^{II}(bpc)₂]⁰-PtO_x/WO₃ system. This value exceeds the representative Z-scheme water splitting systems reported using SrTiO₃:Rh-based H₂-evolving photocatalyst (4.2%³¹ at 420 nm for Ru/SrTiO₃:Rh-Fe^{3+/2+}-BiVO₄) and is also the highest level among those using other photocatalysts without the aid of CrO_x shells. Under simulated sunlight irradiation, the solar-to-hydrogen conversion efficiency reached 0.07% at pH 3.5 and 0.09% at pH 2.0 (Figures 5c and S7).

In summary, a strategy for manipulating the electrostatic interactions between the photocatalyst surface and redox

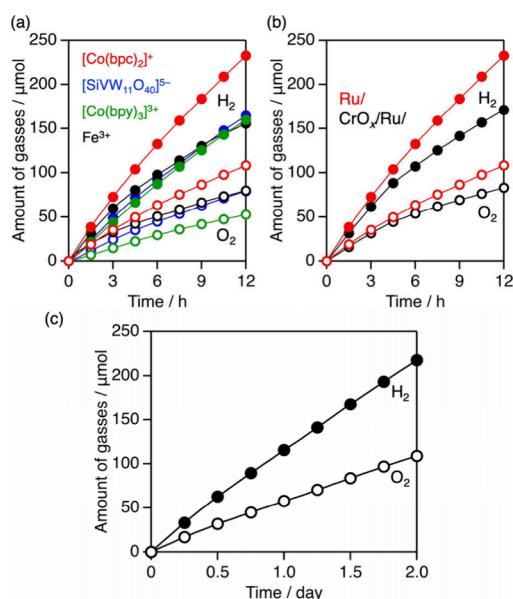


Figure 5. Time courses of Z-scheme water splitting: (a) Ru/SrTiO₃:Rh (60 mg) and PtO_x/WO₃ (80 mg) dispersed in an aqueous solution (pH 2.0, 70 mL) containing various mediators (each 0.3 mM) was irradiated with 405 nm light. (b) CrO_x/Ru/SrTiO₃:Rh or Ru/SrTiO₃:Rh (60 mg) and PtO_x/WO₃ (80 mg) dispersed in an aqueous solution (pH 2.0, 70 mL) containing [Co^{III}(bpc)₂]⁺ (0.3 mM) was irradiated with 405 nm light. (c) Ru/SrTiO₃:Rh (60 mg) and PtO_x/WO₃ (80 mg) dispersed in an aqueous solution (pH 3.5, 70 mL) containing [Co^{III}(bpc)₂]⁺ (0.3 mM) was irradiated under simulated sunlight (AM1.5G, 100 mW cm⁻², irradiation area of 5.76 cm²).

mediators was introduced to suppress undesirable backward electron transfer, even without the aid of the widely applied CrO_x shell. The designed, charge-switchable cobalt complex [Co^{III}(bpc)₂]⁺/[Co^{II}(bpc)₂]⁰ effectively suppressed backward electron transfer competing with H₂ evolution by electrostatic repulsion against a positively charged SrTiO₃:Rh photocatalyst, maintaining undisturbed forward electron transfer. The best combination of the chromium-free Ru/SrTiO₃:Rh H₂-evolving photocatalyst, [Co^{III}(bpc)₂]⁺/[Co^{II}(bpc)₂]⁰ mediator, and WO₃-based O₂-evolving photocatalyst provided superior overall Z-scheme water splitting compared to those using any CrO_x-free H₂-evolving photocatalyst or other conventional electron mediators, with an AQY of 7.2% at 405 nm and an STH of 0.09%. We believe that the strategy developed in this study provides a guideline for efficient solar water splitting without the use of potentially toxic chromium modifications, which is essential for practical applications.

■ ASSOCIATED CONTENT

Supporting Information

The Supporting Information is available free of charge at <https://pubs.acs.org/doi/10.1021/jacs.5c23111>.

Experimental procedures, cyclic voltammograms, X-ray diffraction patterns, UV–vis diffuse reflectance spectra, photocatalytic activities, and results of ICP-OES (PDF)

■ AUTHOR INFORMATION

Corresponding Authors

Akinobu Nakada – Department of Energy and Hydrocarbon Chemistry, Graduate School of Engineering, Kyoto University,

Kyoto 615-8510, Japan; orcid.org/0000-0001-6670-5044; Email: nakada@scl.kyoto-u.ac.jp

Ryu Abe – Department of Energy and Hydrocarbon Chemistry, Graduate School of Engineering, Kyoto University, Kyoto 615-8510, Japan; orcid.org/0000-0001-8592-076X; Email: ryu-abe@scl.kyoto-u.ac.jp

Authors

Ren Itagaki – Department of Energy and Hydrocarbon Chemistry, Graduate School of Engineering, Kyoto University, Kyoto 615-8510, Japan

Hajime Suzuki – Department of Energy and Hydrocarbon Chemistry, Graduate School of Engineering, Kyoto University, Kyoto 615-8510, Japan; Precursory Research for Embryonic Science and Technology (PRESTO), Japan Science and Technology Agency (JST), Kawaguchi, Saitama 332-0012, Japan; orcid.org/0000-0002-8891-2033

Osamu Tomita – Department of Energy and Hydrocarbon Chemistry, Graduate School of Engineering, Kyoto University, Kyoto 615-8510, Japan; orcid.org/0000-0002-5910-8732

Complete contact information is available at: <https://pubs.acs.org/10.1021/jacs.5c23111>

Notes

The authors declare no competing financial interest.

■ ACKNOWLEDGMENTS

This work was supported by a JSPS KAKENHI grant (JP24K01603) and a Grant-in-Aid for Transformative Research Areas “Concerto Photocatalysis” (JP23H03830 and JP23H03832). R.I. wishes to acknowledge the support from JSPS Fellowship for Young Scientists (JP23KJ1351). We would like to express our gratitude to Mr. Harutaka Ninomiya for his assistance with the synthesis of the polyoxometalates.

■ REFERENCES

- (1) Kudo, A.; Miseki, Y. Heterogeneous photocatalyst materials for water splitting. *Chem. Soc. Rev.* **2009**, *38*, 253–278.
- (2) Abe, R. Development of a New System for Photocatalytic Water Splitting into H₂ and O₂ under Visible Light Irradiation. *Bull. Chem. Soc. Jpn.* **2011**, *84*, 1000–1030.
- (3) Chen, S.; Takata, T.; Domen, K. Particulate photocatalysts for overall water splitting. *Nat. Rev. Mater.* **2017**, *2*, 17050.
- (4) Wang, Y.; Suzuki, H.; Xie, J.; Tomita, O.; Martin, D. J.; Higashi, M.; Kong, D.; Abe, R.; Tang, J. Mimicking Natural Photosynthesis: Solar to Renewable H₂ Fuel Synthesis by Z-Scheme Water Splitting Systems. *Chem. Rev.* **2018**, *118*, 5201–5241.
- (5) Wang, Q.; Domen, K. Particulate Photocatalysts for Light-Driven Water Splitting: Mechanisms, Challenges, and Design Strategies. *Chem. Rev.* **2020**, *120*, 919–985.
- (6) Tao, X.; Zhao, Y.; Wang, S.; Li, C.; Li, R. Recent advances and perspectives for solar-driven water splitting using particulate photocatalysts. *Chem. Soc. Rev.* **2022**, *51*, 3561–3608.
- (7) Shi, M.; Wu, X.; Zhao, Y.; Li, R.; Li, C. Unlocking the Key to Photocatalytic Hydrogen Production Using Electronic Mediators for Z-Scheme Water Splitting. *J. Am. Chem. Soc.* **2025**, *147*, 3641–3649.
- (8) Matsuoka, H.; Inoue, T.; Suzuki, H.; Tomita, O.; Nozawa, S.; Nakada, A.; Abe, R. Surface Modification with Metal Hexacyanoferrates for Expanding the Choice of H₂-Evolving Photocatalysts for Both Fe³⁺/Fe²⁺ Redox-Mediated and Interparticle Z-Scheme Water-Splitting Systems. *Solar RRL* **2023**, *7*, No. 2300431.
- (9) Kato, H.; Sasaki, Y.; Iwase, A.; Kudo, A. Role of Iron Ion Electron Mediator on Photocatalytic Overall Water Splitting under

Visible Light Irradiation Using Z-Scheme Systems. *Bull. Chem. Soc. Jpn.* **2007**, *80*, 2457–2464.

(10) Nakada, A.; Suzuki, H.; Vequizo, J. J. M.; Ogawa, K.; Higashi, M.; Saeki, A.; Yamakata, A.; Kageyama, H.; Abe, R. Fe/Ru Oxide as Versatile and Effective Cocatalyst for Boosting Z-Scheme Water Splitting: Suppressing Undesirable Backward Electron Transfer. *ACS Appl. Mater. Interfaces* **2019**, *11*, 45606–45611.

(11) Suzuki, H.; Okada, Y.; Kise, S.; Sui, X.; Nozawa, S.; Tomita, O.; Abe, R. Core–Shell Structured Cocatalysts for Enhancing Redox-Mediated Z-Scheme Photocatalytic Water Splitting and Producing H₂ and O₂ Separately. *ACS Catal.* **2025**, *15*, 4870–4879.

(12) Li, H.; Vequizo, J. J. M.; Hisatomi, T.; Nakabayashi, M.; Xiao, J.; Tao, X.; Pan, Z.; Li, W.; Chen, S.; Wang, Z.; et al. Zr-doped BaTaO₂N photocatalyst modified with Na–Pt cocatalyst for efficient hydrogen evolution and Z-scheme water splitting. *EES Catal.* **2023**, *1*, 26–35.

(13) Qi, Y.; Chen, S.; Cui, J.; Wang, Z.; Zhang, F.; Li, C. Inhibiting competing reactions of iodate/iodide redox mediators by surface modification of photocatalysts to enable Z-scheme overall water splitting. *Appl. Catal., B* **2018**, *224*, 579–585.

(14) Qureshi, M.; Shinagawa, T.; Tsiapis, N.; Takanabe, K. Exclusive Hydrogen Generation by Electrocatalysts Coated with an Amorphous Chromium-Based Layer Achieving Efficient Overall Water Splitting. *ACS Sustainable Chem. Eng.* **2017**, *5*, 8079–8088.

(15) Yoshino, S.; Kurutach, T.; Liu, Q.; Yamanaka, T.; Nozawa, S.; Kobayashi, M.; Kumagai, H.; Kato, H. Z-scheme water splitting utilizing CuLi_{1/3}Ti_{2/3}O₂ as a hydrogen-evolving photocatalyst with photo-response up to 600 nm. *Sustainable Energy & Fuels* **2024**, *8*, 1260–1268.

(16) Yoshida, M.; Takanabe, K.; Maeda, K.; Ishikawa, A.; Kubota, J.; Sakata, Y.; Ikezawa, Y.; Domen, K. Role and Function of Noble-Metal/Cr-Layer Core/Shell Structure Cocatalysts for Photocatalytic Overall Water Splitting Studied by Model Electrodes. *J. Phys. Chem. C* **2009**, *113*, 10151–10157.

(17) Maeda, K.; Teramura, K.; Lu, D.; Saito, N.; Inoue, Y.; Domen, K. Noble-metal/Cr₂O₃ core/shell nanoparticles as a cocatalyst for photocatalytic overall water splitting. *Angew. Chem., Int. Ed.* **2006**, *45*, 7806–7809.

(18) Takata, T.; Jiang, J.; Sakata, Y.; Nakabayashi, M.; Shibata, N.; Nandal, V.; Seki, K.; Hisatomi, T.; Domen, K. Photocatalytic water splitting with a quantum efficiency of almost unity. *Nature* **2020**, *581*, 411–414.

(19) Li, W.; Li, H.; Ma, Y.; Xiao, J.; Lu, D.; Hisatomi, T.; Domen, K. Enhanced Z-scheme water splitting at atmospheric pressure with suppression of reverse reactions using Zr-doped BaTaO₂N as hydrogen evolution photocatalyst. *J. Catal.* **2023**, *428*, 115187.

(20) Pourbaix, M. *Atlas of Electrochemical Equilibria in Aqueous Solutions*; National Association of Corrosion Engineers, 1974.

(21) Ohno, T.; Bai, L.; Hisatomi, T.; Maeda, K.; Domen, K. Photocatalytic water splitting using modified GaN:ZnO solid solution under visible light: long-time operation and regeneration of activity. *J. Am. Chem. Soc.* **2012**, *134*, 8254–8259.

(22) Lyu, H.; Hisatomi, T.; Goto, Y.; Yoshida, M.; Higashi, T.; Katayama, M.; Takata, T.; Minegishi, T.; Nishiyama, H.; Yamada, T.; et al. An Al-doped SrTiO₃ photocatalyst maintaining sunlight-driven overall water splitting activity for over 1000 h of constant illumination. *Chem. Sci.* **2019**, *10*, 3196–3201.

(23) Sasaki, Y.; Iwase, A.; Kato, H.; Kudo, A. The effect of cocatalyst for Z-scheme photocatalysis systems with an Fe³⁺/Fe²⁺ electron mediator on overall water splitting under visible light irradiation. *J. Catal.* **2008**, *259*, 133–137.

(24) Miseki, Y.; Fujiyoshi, S.; Gunji, T.; Sayama, K. Photocatalytic Z-Scheme Water Splitting for Independent H₂/O₂ Production via a Stepwise Operation Employing a Vanadate Redox Mediator under Visible Light. *J. Phys. Chem. C* **2017**, *121*, 9691–9697.

(25) Pan, Z.; Vequizo, J. J. M.; Yoshida, H.; Li, J.; Zheng, X.; Chu, C.; Wang, Q.; Cai, M.; Sun, S.; Katayama, K.; et al. Simultaneous Structural and Electronic Engineering on Bi- and Rh-co-doped SrTiO₃

for Promoting Photocatalytic Water Splitting. *Angew. Chem., Int. Ed.* **2025**, *64*, No. e202414628.

(26) Bolts, J. M.; Wrighton, M. S. Correlation of photocurrent-voltage curves with flat-band potential for stable photoelectrodes for the photoelectrolysis of water. *J. Phys. Chem.* **1976**, *80*, 2641–2645.

(27) Tomita, O.; Naito, H.; Nakada, A.; Higashi, M.; Abe, R. Mono-transition-metal-substituted polyoxometalates as shuttle redox mediator for Z-scheme water splitting under visible light. *Sustainable Energy & Fuels* **2022**, *6*, 664–673.

(28) Kato, H.; Hori, M.; Kanta, R.; Shimodaira, Y.; Kudo, A. Construction of Z-scheme Type Heterogeneous Photocatalysis Systems for Water Splitting into H₂ and O₂ under Visible Light Irradiation. *Chem. Lett.* **2004**, *33*, 1348–1349.

(29) Sasaki, Y.; Kato, H.; Kudo, A. [Co(bpy)₃]^{3+/2+} and [Co(phen)₃]^{3+/2+} electron mediators for overall water splitting under sunlight irradiation using Z-scheme photocatalyst system. *J. Am. Chem. Soc.* **2013**, *135*, 5441–5449.

(30) Liu, F.; Deng, J.; Su, B.; Peng, K.-S.; Liu, K.; Lin, X.; Hung, S.-F.; Chen, X.; Lu, X. F.; Fang, Y.; et al. Poly(triazine imide) Crystals for Efficient CO₂ Photoreduction: Surface Pyridine Nitrogen Dominates the Performance. *ACS Catal.* **2025**, *15*, 1018–1026.

(31) Kato, H.; Sasaki, Y.; Shirakura, N.; Kudo, A. Synthesis of highly active rhodium-doped SrTiO₃ powders in Z-scheme systems for visible-light-driven photocatalytic overall water splitting. *J. Mater. Chem. A* **2013**, *1*, 12327–12333.